

Dynamic response simulation through system identification

D.E. Roberts^{a,*}, N.C. Hay^b

^aCentre for Mathematics and Statistics, Napier University, 10 Colinton Road, Edinburgh, EH10 5DT, UK

^bSchool of Engineering, Napier University, 10 Colinton Road, Edinburgh, EH10 5DT, UK

Received 28 April 2005; received in revised form 12 December 2005; accepted 8 February 2006

Available online 27 April 2006

Abstract

Nonlinear dynamic systems, such as those associated with structural testing of vehicles, are considered. The vehicle, or a substructure, is mounted in a test rig that is normally driven by servo-hydraulic actuators. The specimen and test rig form a nonlinear dynamic system. These test systems assure the durability of vehicles by reproducing a structural response time history that has been measured in a road test of a vehicle. For this, a force or displacement input to the actuators' control system must be determined as a function of time.

Current practice employs an iterative algorithm, using a frequency response function to represent the system. The conventional iteration is a particular version of well established numerical techniques for solving nonlinear systems. However, the success of the iteration is dependent on the degree of nonlinearity and on the level of noise in the signals coming from the system.

This paper advocates identifying the system to improve its representation in the iterative algorithm. The theory underpinning the alternative algorithm is presented and a comparison is made between the performances of the two algorithms, using computer simulations based on Duffing's equation. These simulations show that, even for this simple model, the alternative algorithm is faster, more reliable and more tolerant of response noise.

© 2006 Elsevier Ltd. All rights reserved.

1. Introduction

The situation addressed in this paper is described in Ref. [1] which discusses methods for determining the force input as a function of time, known as a 'drive file', to a nonlinear dynamic system such that a specified response history is reproduced. This occurs in laboratory simulation testing of vehicles in which a response that is measured during road testing must be reproduced in the laboratory by a specially constructed test rig. In Ref. [1] it is explained how the conventional algorithm developed in the 1970s—see e.g. Ref. [2]—may be viewed as an instance of more general numerical algorithms for solving nonlinear equations, Newton's method being the most well known.

In application, the system is not known explicitly. However, the system can be modelled by measuring a frequency response function by applying a known excitation and measuring the subsequent response. This function is used in two ways. It is employed in estimating the initial drive file and in forming an approximate

*Corresponding author. Fax: +1 31 455 7122.

E-mail addresses: d.roberts@napier.ac.uk (D.E. Roberts), n.hay@napier.ac.uk (N.C. Hay).

Jacobian for use in numerical techniques. The conventional laboratory simulation algorithm uses this linear estimation as a constant Jacobian in an iteration to determine the updated drive file. An alternative method, due to Broyden [3–5], was also described in Ref. [1]. In the latter technique, the Jacobian is progressively updated. Roberts and Hay [1] also discuss search methods leading to a determination of the iteration gain.

The conventional and Broyden's method were found to be of limited success in experiments using a mathematical simulation based on Duffing's equation in situations of high nonlinearity. The performance deteriorated in additional numerical experiments in which the data were corrupted by noise, as is inevitably the case in practice. The work for Ref. [1] led the authors to believe that it was the representation of the system that was crucial to the performance of the iterative algorithm and that system identification should be examined. Techniques for system identification can be found, for example, in Ref. [6].

In the following, the framework for discussing and testing the algorithms is reconstructed. The conventional and Broyden's method are then described. The shortcomings of these algorithms under high nonlinearity and in the presence of noise is demonstrated using a one degree of freedom damped spring–mass system containing a nonlinear spring and represented by Duffing's equation. To illustrate the approach advocated in this paper, a simple, readily implemented method of system identification, which involves the idea of frequency response functions, is then described and applied under similar circumstances of high nonlinearity and noise corrupted signals. The method is shown to be a significant improvement over the earlier approaches.

2. Framework for numerical techniques

A given nonlinear system is excited by a signal represented by the components of a vector $\mathbf{x} := (x_0, x_1, \dots, x_{N-1})$. The response is sampled, yielding $\mathbf{y} := (y_0, y_1, \dots, y_{N-1})$, where, for signals of period T , $y_i := y(t_i)$ with $t_i := iT/N$ for $i = 0, 1, \dots, N - 1$. The response vector is a function of the input signal:

$$\mathbf{y} = \mathbf{f}(\mathbf{x}), \quad (1)$$

or, in component form:

$$\left. \begin{aligned} y_0 &= f_0(x_0, x_1, \dots, x_{N-1}) \\ y_1 &= f_1(x_0, x_1, \dots, x_{N-1}) \\ &\vdots \\ y_{N-1} &= f_{N-1}(x_0, x_1, \dots, x_{N-1}) \end{aligned} \right\} \quad (2)$$

The problem considered in this paper is, given a particular response \mathbf{y}^D , determine an input signal which induces this response. That is, solve the following vector equation for \mathbf{x} :

$$\mathbf{f}(\mathbf{x}) - \mathbf{y}^D = \mathbf{0}. \quad (3)$$

Here, the target response comes from exciting the system using band-limited white noise. Portions of a typical excitation and target response are shown in Fig. 1 for a nonlinearity coefficient $k' = 0.4$, c.f. Eq. (9).

The system of Eqs. (3) may be solved numerically using iterative methods that are variations of Newton's method for many variables—for example Refs. [3–5]

$$\mathbf{x}^{(n+1)} := \mathbf{x}^{(n)} + \lambda_n \mathbf{p}^{(n)}, \quad (4)$$

where $\mathbf{p}^{(n)}$ is given by

$$\mathbf{p}^{(n)} := [B_n]^{-1} [\mathbf{y}^D - \mathbf{y}^{(n)}] \quad (5)$$

and the λ_n , for $n = 0, 1, \dots$ are real numbers lying between 0 and 1. The matrix B_n is an approximation to the Jacobian $J_{\mathbf{f}}(\mathbf{x}^{(n)})$ of the vector-valued function \mathbf{f} evaluated at $\mathbf{x}^{(n)}$:

$$[J_{\mathbf{f}}(\mathbf{x})]_{i,j} := \frac{\partial y_i}{\partial x_j} \quad \text{for } i, j = 0, 1, \dots, N - 1, \quad (6)$$

in which the partial derivatives are evaluated at \mathbf{x} .

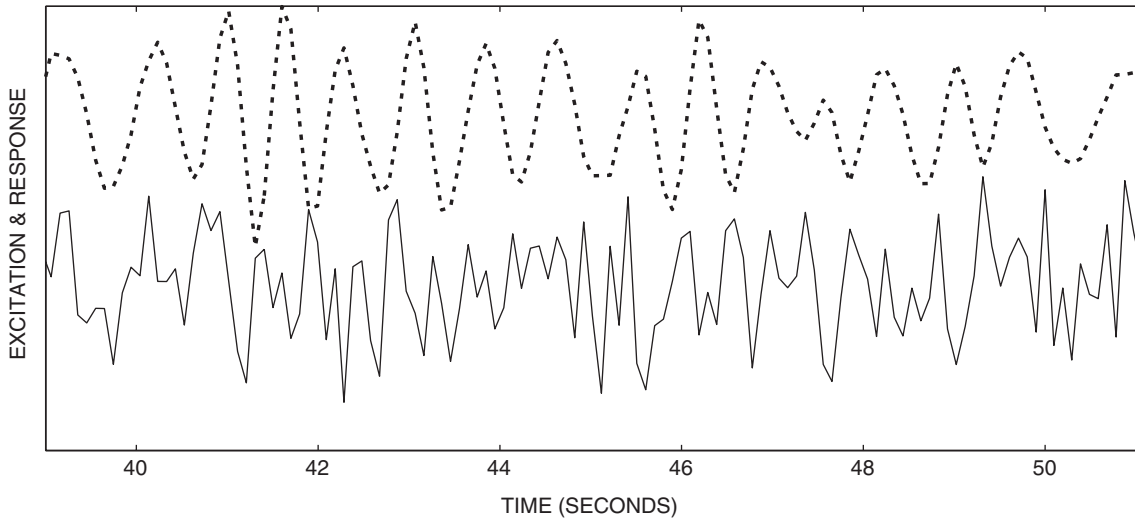


Fig. 1. Typical drive and response signals against time for $k' = 0.4$ with 5% noise. Dashed line—the specified response; solid line—the excitation to be determined.

A sequence of excitation vectors $\mathbf{x}^{(n)}$ for $n = 0, 1, \dots$ is produced for which the corresponding response vectors $\mathbf{y}^{(n)}$, hopefully converge to \mathbf{y}^D . The iteration is stopped when the fractional Euclidean norm of the error vector, given in Eqs. (7) and (8), falls below a prescribed tolerance (tol).

$$|\mathbf{e}y^{(n)}|/|\mathbf{y}^D| < \text{tol}, \tag{7}$$

where

$$\mathbf{e}y^{(n)} := \mathbf{y}^D - \mathbf{y}^{(n)}. \tag{8}$$

The success of these methods depends on how close the initial excitation $\mathbf{x}^{(0)}$ is to the solution and on the accuracy of the approximation B_n . Both of these aspects depend on how well the function \mathbf{f} is represented.

3. The nonlinear system

Numerical experiments comparing approaches were conducted using a model problem consisting of a nonlinear spring as furnished by Duffing's equation:

$$m \frac{d^2y(t)}{dt^2} + c \frac{dy(t)}{dt} + ky(t)[1 + k'y(t)^2] = kx(t), \tag{9}$$

subject to the initial conditions $y(0) = \dot{y}(0) = 0$.

The mass is taken to be 100 kg, and the natural frequency (in Hz) ($f_n = 1/2\pi\sqrt{k/m}$ of the linear system, when $k' = 0$) is taken as unity. Similarly, the damping coefficient 'c' is defined by choosing a damping ratio of the linear system as 0.1.

An effective frequency response function of this system is measured by a spectral analyser which averages over 10 frames of data. Examples of this function are shown in Fig. 2 for a nonlinearity coefficient, k' , of value 0.4 using band-limited random noise. One is measured at an excitation level with a standard deviation of unity, while in the other, the standard deviation is 0.1 to reduce the effect of the nonlinearity in the spring. Both include 5% noise.

As in Ref. [1], the frequency response function is smoothed using a least squares fit to produce a rational function which has as numerator a linear polynomial and as denominator a quadratic polynomial in frequency. The effect of the nonlinearity may be seen from this graph. Note that, for low amplitudes, spectral

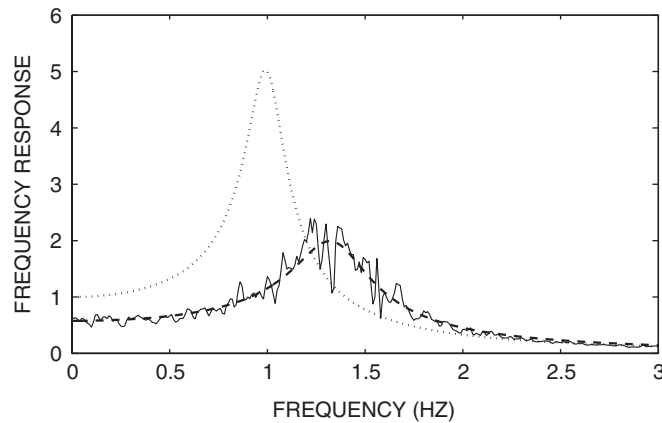


Fig. 2. Frequency response functions for $k' = 0.4$ and 5% noise using 10 frames to average. The dotted line is a plot of the measurement at an amplitude of 0.1 and of $|\mathbf{H}^{\text{lin}}|$ itself. The solid line is the measurement at an amplitude of 1.0 before smoothing. The dashed line is the smoothed measurement at amplitude 1.0.

analysis yields a good approximation to the ($k' = 0$) linear response, \mathbf{H}^{lin} —see Eq. (16). Fig. 2 also shows $|\mathbf{H}^{\text{lin}}|$, but it is indistinguishable from the system measured at low amplitude.

4. Application of conventional algorithm and related schemes

In the conventional algorithm, the system is treated as linear, i.e.,

$$\mathbf{y} = \mathbf{f}(\mathbf{x}) \approx \mathbf{h} * \mathbf{x}, \tag{10}$$

in which the measured impulse response is denoted by \mathbf{h} . The convolution may be replaced by a matrix multiplication $\mathbf{y} = C_h \mathbf{x}$ where C_h is the $N \times N$ circulant matrix:

$$C_h = \begin{bmatrix} h_0 & h_{N-1} & h_{N-2} & \dots & h_1 \\ h_1 & h_0 & h_{N-1} & \dots & h_2 \\ \vdots & & & & \\ h_{N-1} & h_{N-2} & h_{N-3} & \dots & h_0 \end{bmatrix}. \tag{11}$$

Hence, the approximation to the Jacobian is a constant matrix:

$$B_n := C_h, \quad n = 0, 1, 2, \dots \tag{12}$$

The initial excitation is given by

$$\mathbf{x}^{(0)} := \mathbf{f}^{-1}(\mathbf{y}^D) = C_h^{-1} \mathbf{y}^D. \tag{13}$$

The conventional iteration follows Eq. (4) in which λ is set by the operator.

In Broyden’s method, the same initial input is employed, but the estimate of the Jacobian is updated on each iteration starting from $B_0 = C_h$. Again, the gain is set by the operator, or, to aid global convergence, a search method may be used to determine an optimal value—see Ref. [1] for more details.

The efficacy of the above methods is demonstrated using the Duffing model. Fig. 3 illustrates the convergence of the iterations based on the conventional algorithm and on Broyden’s method for a nonlinear coefficient of $k' = 0.3$ and an iteration gain factor of 0.5.

When the nonlinearity, k' , is increased above 0.4, and no noise is present, neither method converges for an iteration gain of 0.5. In industrial practice, the gain is then adjusted by the operator to facilitate convergence, if possible. Plots corresponding to an iteration gain of 0.2 are included in Fig. 4. Not surprisingly, when noise corrupts the response, the convergence is further compromised.

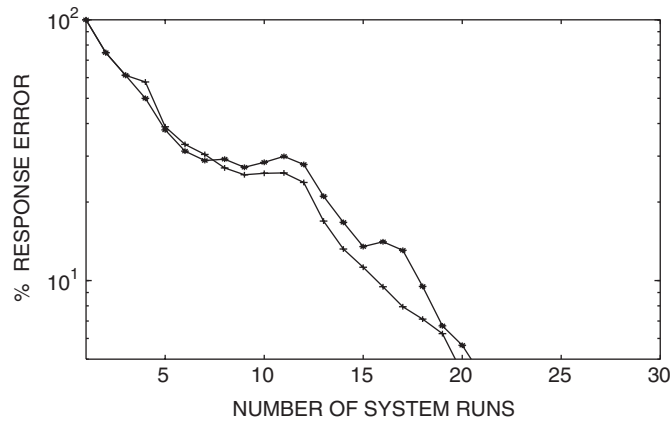


Fig. 3. The fractional error in the response as a function of the number of system runs, both for the conventional (*) and Broyden (+) methods. The nonlinear coefficient is $k' = 0.3$. There is no noise and the iteration gain is 0.5.

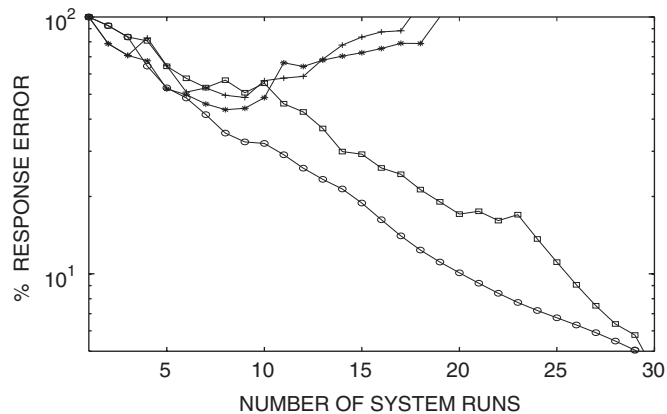


Fig. 4. The fractional error in the response as a function of the number of system runs, both for the conventional (*) and Broyden (+) methods with an iteration gain of 0.5. Also plotted are the results when the gain is reduced to 0.2—conventional (open circle) and Broyden (box). All for $k' = 0.4$ and no noise.

5. System identification

These iterative schemes are now shown to be improved by determining a better approximation to the vector-valued function \mathbf{f} , rather than using the approximation (10), which is based on the effective impulse response \mathbf{h} obtained by regarding the system as linear.

A more accurate representation of \mathbf{f} may be achieved by identifying the system. There is a large body of literature on system identification—see, for example, Ref. [6] for references. However, the aim of this paper is to demonstrate the advantages of employing system identification techniques in the algorithms applied to the testing of dynamic systems in the laboratory. In order to keep the presentation self-contained and transparent, a straightforward form of system identification is adopted. The approach involves the use of frequency response ideas which are employed in the conventional algorithm. This works for the simple model described earlier and is readily implemented. For higher dimensional systems with more complex nonlinearities, resort may be made to more appropriate techniques of system identification. The only requirements are that the method used generates an approximation to the inverse function \mathbf{f}^{-1} and the corresponding Jacobian, as in Eqs. (20) and (22).

The method used in this paper starts from the observation that discretisation of the differential equation (9), leads to the approximation:

$$kx_i = [m\ddot{y} + c\dot{y} + ky(1 + k'y^2)]_{t=t_i} \approx k[Cy]_i + kk'y_i^3, \tag{14}$$

in which C is a circulant matrix, such that the i th component of the discrete Fourier transform of the vector $[Cy]$ is given by

$$\frac{Y_i}{H_i^{\text{lin}}}, \tag{15}$$

where H^{lin} is the transform corresponding to the discretised version of

$$\frac{k}{-\omega^2m + j\omega c + k}, \tag{16}$$

at the discrete frequencies $\omega_l := 2\pi l/T$ for $l = 0, 1, \dots, N/2$.

This yields the relationship:

$$\mathbf{x} = C\mathbf{y} + \mathbf{g}(\mathbf{y}) = \mathbf{f}^{-1}(\mathbf{y}), \tag{17}$$

where $[\mathbf{g}(\mathbf{y})]_i := k'y_i^3$. Thus the detail of the model yields an explicit form for the *function inverse* of \mathbf{f} .

Indeed, consideration of the model problem leads to an *approximation* of the function \mathbf{f}^{-1} consisting of *two* operations. Firstly, the linear part of Eq. (17), characterised by C , may be estimated (yielding a circulant matrix \tilde{C} corresponding to an impulse vector $\tilde{\mathbf{h}}$), by measuring the frequency response function using a *low amplitude* drive (e.g. 10% of full amplitude). The excitation is a band-limited white noise random signal. Under these conditions the contribution from the nonlinear term $\mathbf{g}(\mathbf{y})$ is relatively small. The modulus of the measured frequency response and that of H^{lin} are plotted in Fig. 5 for $k' = 0.4$ and noise level of 5%.

To estimate the nonlinear part of the system $\mathbf{g}(\mathbf{y})$, a higher amplitude drive signal, \mathbf{x} , is chosen and the response \mathbf{y} recorded. The nonlinear term in Eq. (17) may be isolated and then approximated by observing the following relation between input and output:

$$[\mathbf{x} - C\mathbf{y}]_i = k'y_i^3. \tag{18}$$

The higher amplitude drive may be chosen to be band-limited white noise, noise with a shaped spectrum, for example $1/f$, or a simpler input such as a sinusoid of a suitable amplitude and frequency. To obtain a more accurate approximation of the nonlinearity, especially if white noise is chosen, five runs are repeated using the same input. The responses are then averaged. An example of $[\mathbf{x} - \tilde{C}\mathbf{y}]_i$ plotted against y_i for $i = 0, 1, \dots, N - 1$, is presented in Fig. 6 for the system of Eqs. (17) with $k' = 0.4$, no noise present and the system excited by a sinusoid whose amplitude is 2.0 and whose frequency is 1.4 Hz.

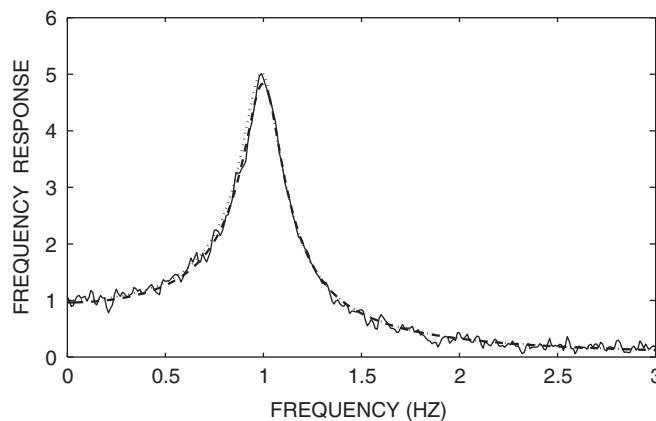


Fig. 5. Plot of the magnitude of frequency response functions for $k' = 0.4$ and noise of 5%. The solid line is the function measured at amplitude 0.1. The dashed line is the smoothed function using least squares. The dotted line is that of $|H^{\text{lin}}|$.

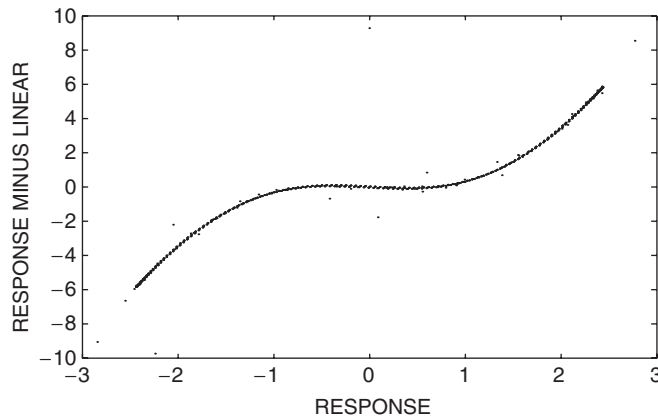


Fig. 6. Estimation of nonlinearity for $k' = 0.4$ using a sinusoid of amplitude 2.0 and frequency of 1.4 Hz with no noise—full record with outliers.

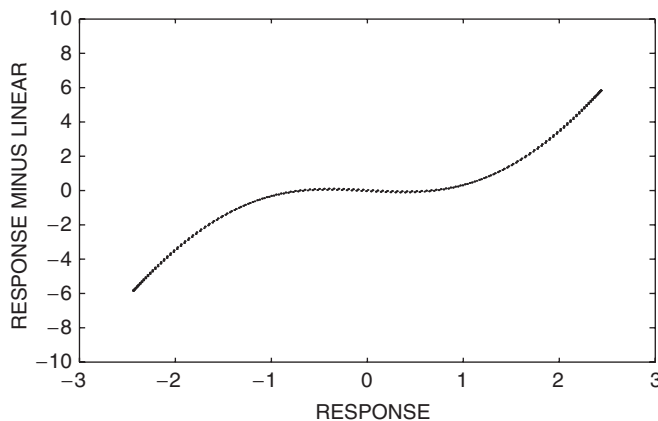


Fig. 7. Estimation of nonlinearity for $k' = 0.4$ using a sinusoid of amplitude 2.0 and frequency of 1.4 Hz with no noise—reduced record which removes outliers.

Outliers, or stray points, are apparent due to the discontinuity in the response arising from the discrete Fourier transform treating the data as periodic functions. This compromises the estimates of the derivatives in Eq. (14). These outliers may be eliminated by removing the beginning and end parts of the frame of data or by using a suitable window. The resulting data are shown in Fig. 7 and may be used as the basis of a least squares fit. In the results to follow, the full response, including outliers is used.

In the above examples, the system was excited by a sinusoid. Exciting the system with band-limited white noise of constant spectrum provides comparable results. Fig. 8 shows the function identified by such an input. More scatter is apparent since the signal is less smooth throughout the time period.

The cubic nature of the relationship is apparent and a ready estimate of the polynomial may be made using the facilities in MATLAB to perform a least squares fit to produce a vector valued cubic:

$$[\mathbf{q}(\mathbf{y})]_i := a_0 + a_1 y_i + a_2 y_i^2 + a_3 y_i^3. \quad (19)$$

A more rigorous approach may be adopted, which would also check the appropriate polynomial degree, and, in more general circumstances, other approximation methods, such as cubic splines, may be employed.

The predictions of the coefficients of Eq. (19) by sinusoid, with and without outlier removal, and using band-limited white noise, are presented in Table 1.

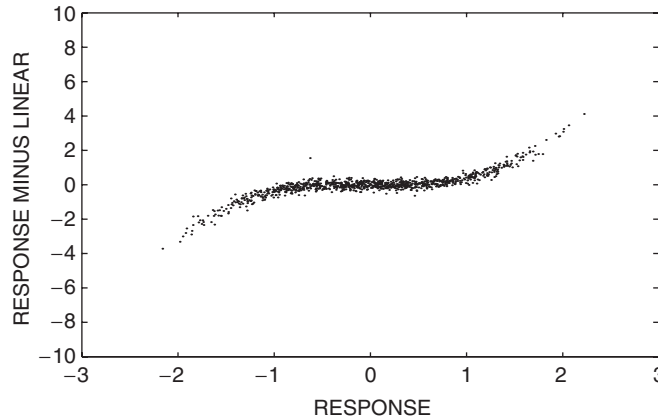


Fig. 8. Estimation of nonlinearity for $k' = 0.4$ and no noise, using a random drive.

Table 1

Table of estimated polynomial coefficients for nonlinearity $k' = 0.4$ and no noise, using random input or sinusoid of (a) full record or (b) reduced record

Coefficient	a_0	a_1	a_2	a_3
Random	0.0032	-0.0385	-0.0023	0.4096
(a) Sine	0.0192	0.0324	-0.0056	0.4084
(b) Sine	0.0004	0.0296	-0.0002	0.4084

Based on the coefficients determined by least squares fit, the following approximation to the system is obtained:

$$\mathbf{x} = \mathbf{f}^{-1}(\mathbf{y}) \approx \tilde{\mathbf{C}}\mathbf{y} + \mathbf{q}(\mathbf{y}), \tag{20}$$

where $\tilde{\mathbf{C}}$ is determined from an estimate of the linear response.

Given the target response \mathbf{y}^D , the initial excitation may be constructed from

$$\mathbf{x}^{(0)} := \tilde{\mathbf{C}}\mathbf{y}^D + \mathbf{q}(\mathbf{y}^D). \tag{21}$$

The Jacobian matrix is now estimated from Eq. (20)

$$[J_{\mathbf{f}}(\mathbf{x})]^{-1} = J_{\mathbf{f}^{-1}}(\mathbf{y}) = \begin{bmatrix} \frac{\partial x_i}{\partial y_j} \end{bmatrix} \approx \tilde{\mathbf{C}} + \mathbf{q}'(\mathbf{y}) =: [\tilde{\mathbf{J}}(\mathbf{x})]^{-1}, \tag{22}$$

where

$$[\mathbf{q}'(\mathbf{y})]_{ij} := [a_1 + 2a_2y_i + 3a_3y_i^2]\delta_{ij}, \tag{23}$$

which only contributes to the diagonal terms.

The iteration scheme described earlier may now be initiated with the starting vector $\mathbf{x}^{(0)}$ and implemented with:

$$\mathbf{B}_n := \tilde{\mathbf{J}}(\mathbf{x}^{(n)}) \tag{24}$$

defined on each iteration. This provides a better starting point and a more accurate Jacobian for the iteration algorithms. This is apparent in Fig. 9 which is comparable to Fig. 4 for the conventional and Broyden methods (note the different scales on the vertical axes).

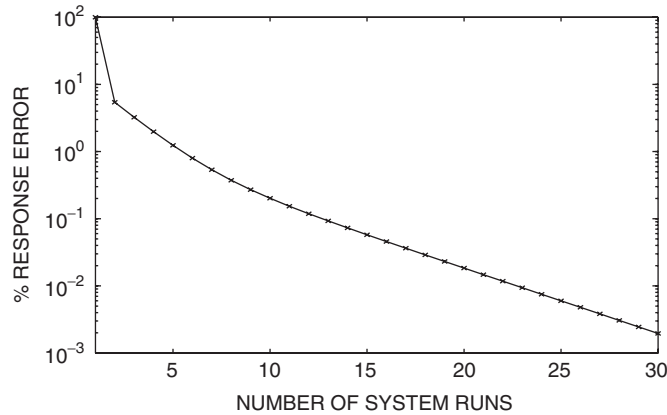


Fig. 9. Fractional error in response using system identification for $k' = 0.4$ and no measurement noise. The drive used to estimate the nonlinearity is band-limited white noise.

Table 2

Table of percentage error in the response for nonlinearity $k' = 0.4$ and no noise, with constant $\lambda = 0.5$

Runs	0	1	2	3	4	5	6	7	8	9
Random	100	5.41	3.24	1.98	1.24	0.80	0.54	0.37	0.27	0.20
(a) Sine	100	9.99	4.93	2.58	1.40	0.78	0.45	0.27	0.16	0.10
(b) Sine	100	9.41	4.69	2.47	1.35	0.75	0.43	0.25	0.16	0.10

Results obtained using (a) full record and (b) reduced record.

A comparison of the convergence using band-limited white noise or a sinusoid to characterise the nonlinearity is presented in Table 2.

6. The effect of noise

In this section, the effect of noise on the measurement of the response \mathbf{y} is considered. The noise level is expressed as the ratio of the rms of the noise signal to the rms of the target response.

The effect of noise on the system identification process of the previous section is illustrated by considering the example of a noise level of 5% and a nonlinearity of 0.4, values for which the conventional algorithms fail. As in the case of no noise, an estimate of the linear part of the Jacobian is made using band-limited noise whose standard deviation is 0.1 of operating levels and smoothed by least squares. Note that a 5% level of noise in the response at full amplitude is equivalent to a 30% noise level at the reduced amplitude.

The system is now excited using a sinusoid of frequency 1.4 Hz and an amplitude of 2.0. To reduce the effect of noise, five runs are repeated using the same input, as for the case of no noise. The responses are then averaged, and estimates of the coefficients of the cubic polynomial are made. For comparison, this procedure is repeated using band-limited white noise. The results of the various ways of estimating the coefficients are presented in Table 3 which shows them to be little different.

The effect of the noise on the estimate of these coefficients is demonstrated by increased scatter in the plot of $[\mathbf{x} - \tilde{\mathbf{C}}\mathbf{y}]_i$ against y_i as shown in Fig. 10 for the application of the sinusoid.

Now that the estimate of the function \mathbf{f}^{-1} has been obtained, the starting value \mathbf{x}_0 is computed from Eq. (21) and the Jacobian from Eq. (24). The iteration of Eqs. (4) and (5) is now implemented. The convergence is illustrated in Table 4 and in Fig. 11. Note that it is impossible to iterate to a tolerance below the level of noise.

The convergence behaviour contrasts with the conventional approach and that using the Broyden update, which two methods fail to converge when noise is present at this level of nonlinearity.

Table 3
Table of estimated polynomial coefficients for nonlinearity $k' = 0.4$ and a noise level of 5%

Coefficient	a_0	a_1	a_2	a_3
Random	0.0022	-0.0408	-0.0036	0.4078
(a) Sine	0.0123	0.0498	-0.0067	0.4018
(b) Sine	-0.0062	0.0887	0.0013	0.3923

Results obtained using (a) full record and (b) reduced record.

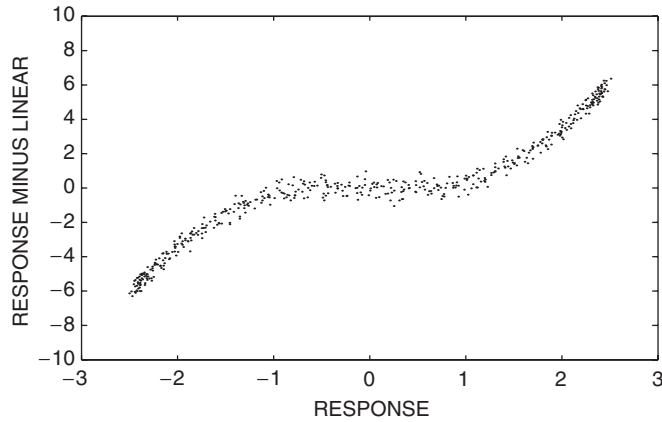


Fig. 10. Plot of $(\mathbf{x} - \tilde{\mathbf{C}}\mathbf{y})_i$ vs y_i for $k' = 0.4$ and 5% noise, using a sinusoid of reduced record.

Table 4
Table of percentage error in the response for nonlinearity $k' = 0.4$ and noise level of 5%, with constant $\lambda = 0.5$

Runs	0	1	2	3	4	5	6	7	8	9
Random	100	9.23	6.65	5.91	6.09	6.01	5.62	5.78	6.15	6.13
(a) Sine	100	16.14	9.28	6.66	6.15	6.05	5.58	5.78	6.13	6.04
(b) Sine	100	18.53	10.62	7.27	6.34	6.15	5.61	5.80	6.16	6.04

Results obtained using (a) full record and (b) reduced record.

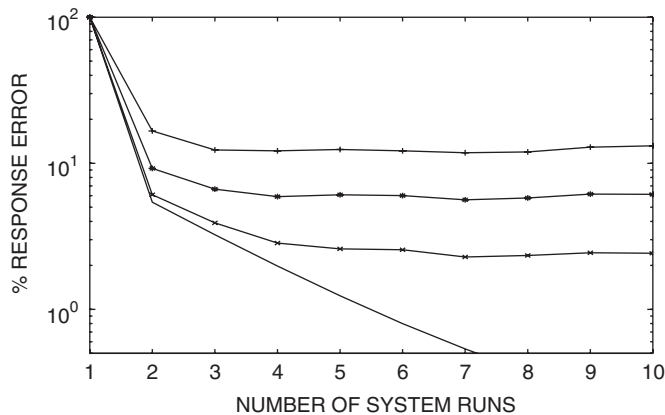


Fig. 11. Results of applying the method using system identification for various levels of noise. The drive used to estimate the nonlinearity, $k' = 0.4$, is band-limited random noise, employing the full record. Noise level: (+) 10%, (*) 5%, (x) 2%, solid line—no noise.

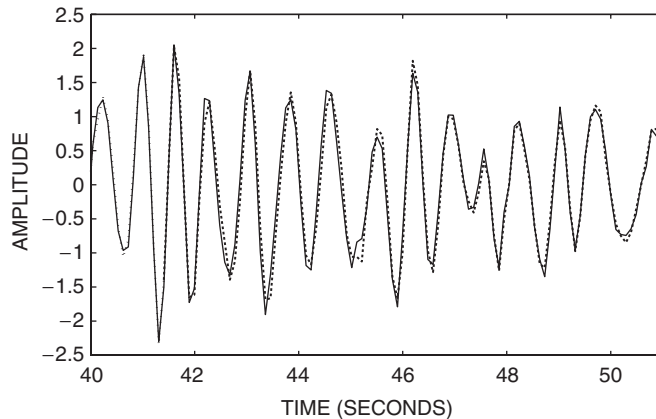


Fig. 12. Part of the desired and achieved response signals using system identification for $k' = 0.4$ and 10% noise. The dotted line represents the desired response. The solid line represents the achieved response.

Fig. 12 compares the desired response and that achieved by the new method for a high level of measurement noise.

7. Conclusions

A method for reproducing a specified response history from a nonlinear dynamic system has been presented. The method has been tested by applying it to a single degree of freedom, nonlinear spring mass system based on a model described by Duffing's equation. Simulations show that the method is substantially better than current iterative methods and is applicable to much higher levels of nonlinearity. In the simulations, it was shown that the method tolerates noise in the response signals from the nonlinear system. Even so, for much higher levels of nonlinearity it may be necessary to reduce the iteration gain or to employ a search method in order to achieve convergence.

In practical situations, the method described here must be developed for application to multiple input–output systems and to other system configurations, such as base excitation. Also, the nonlinearity in Duffing's equation may be simplistic compared to that of a practical system and alternative forms of nonlinearity must be tested. In tackling these more complicated problems, resort may be made to alternative, more sophisticated techniques of system identification.

The work presented in this paper is a consequence of reforming current algorithms in terms of well-established computational techniques and exploring the detail of the model problem. It is clear that the use of system identification in drive file iteration is worthy of further development.

References

- [1] D.E. Roberts, N.C. Hay, Dynamic response simulation for a nonlinear system, *Journal of Sound and Vibration* 281 (2005) 783–798.
- [2] C.J. Dodds, A.R. Plummer, Laboratory road simulation for full vehicle testing—a review, *Symposium of International Automotive Technology*, Pune, India, January 2001 SAE 2001-01-0047.
- [3] J.E. Dennis Jr., R.B. Schnabel, *Numerical Methods for Unconstrained Optimization and Non-linear Equations*, Prentice-Hall, Englewood Cliffs, NJ, 1983.
- [4] C.T. Kelley, *Iterative Methods for Linear and Nonlinear Equations*, SIAM, Philadelphia, PA, 1995.
- [5] J.M. Martinez, Practical quasi-Newton methods for solving nonlinear systems, *Journal of Computational and Applied Mathematics* 124 (2000) 97–121.
- [6] L. Ljung, *Systems Identification: Theory for the User*, Prentice-Hall, Englewood Cliffs, NJ, 1999 (ISBN 0-13-656695-2).